High-mass protostellar jets: a new class of gamma-ray sources

Anabella Araudo[1,2]

(1) ELi - Beamlines, Institute of Physics, Czech Academy of Sciences
(2) Astronomical Institute of the Academy of Sciences, Prague

In collaboration with M. Padovani, A. Marcowith, C. Carrasco-Gonzalez, A. Rodriguez-Kamenetzky, L.F. Rodriguez

Star forming regions

Young Stellar Objects (YSOs)

- Central protostar
- Accretion disc
- Slow outflows
- Fast and collimated jets

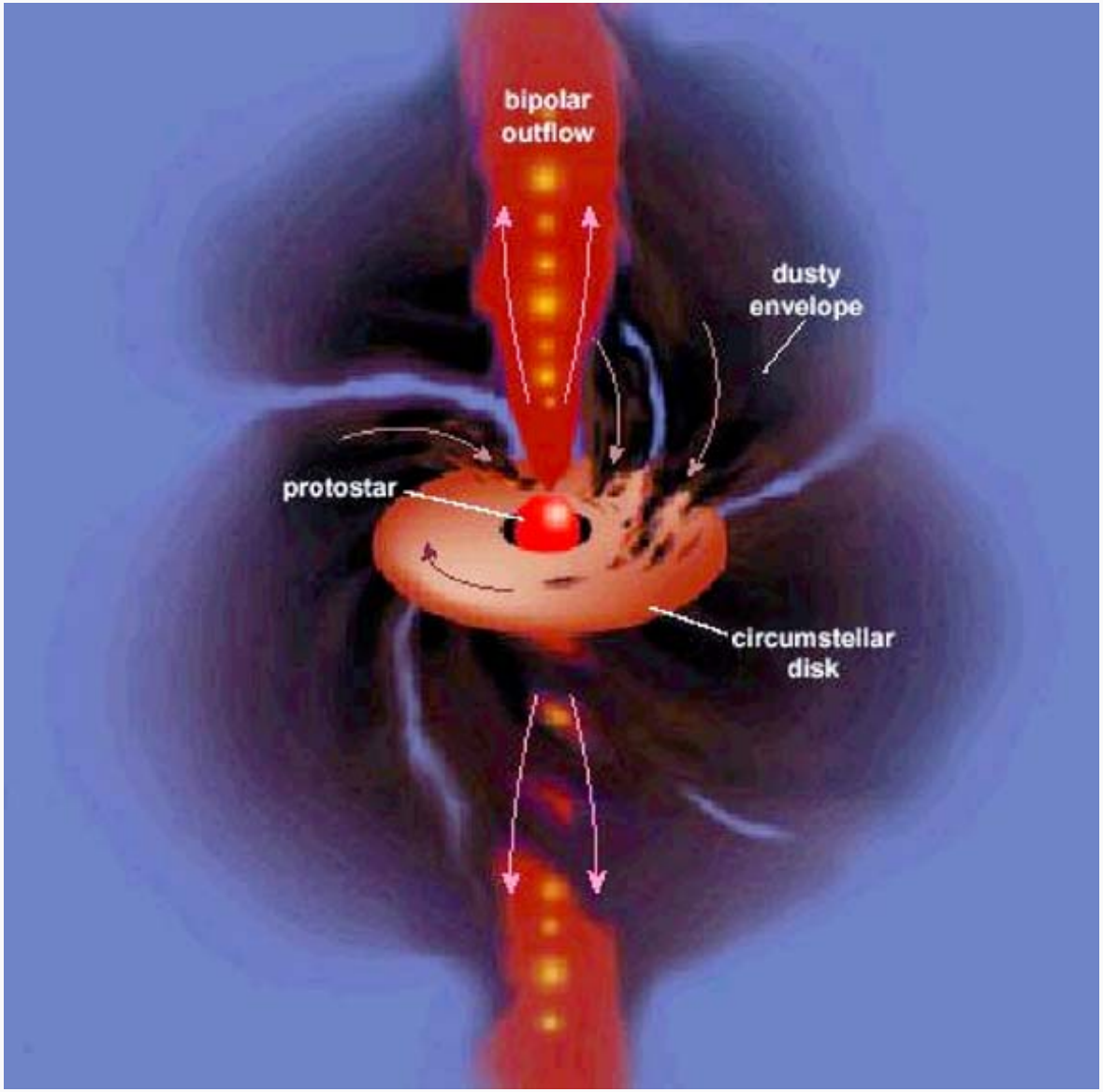

Jet velocity inferred from proper motions

- Low-mass protostars:
  $v_j \sim 50 - 200$ km/s
- High-mass protostars:
  $v_j \sim 200 - 1500$ km/s

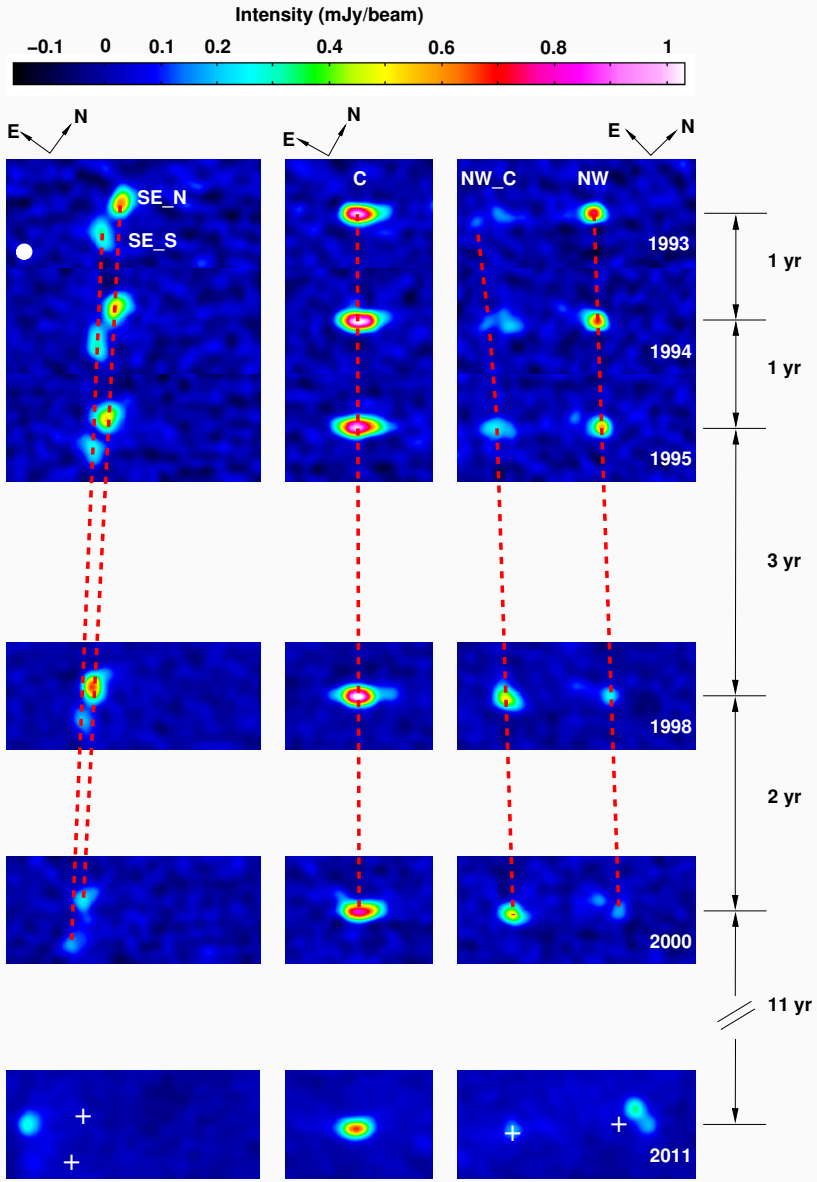

Rodriguez-Kamenetzky et al. (2016)

Protostellar jets

- Well known thermal emitters
- Increasing population of **non-thermal protostellar jets** (Purser et al. 2016)

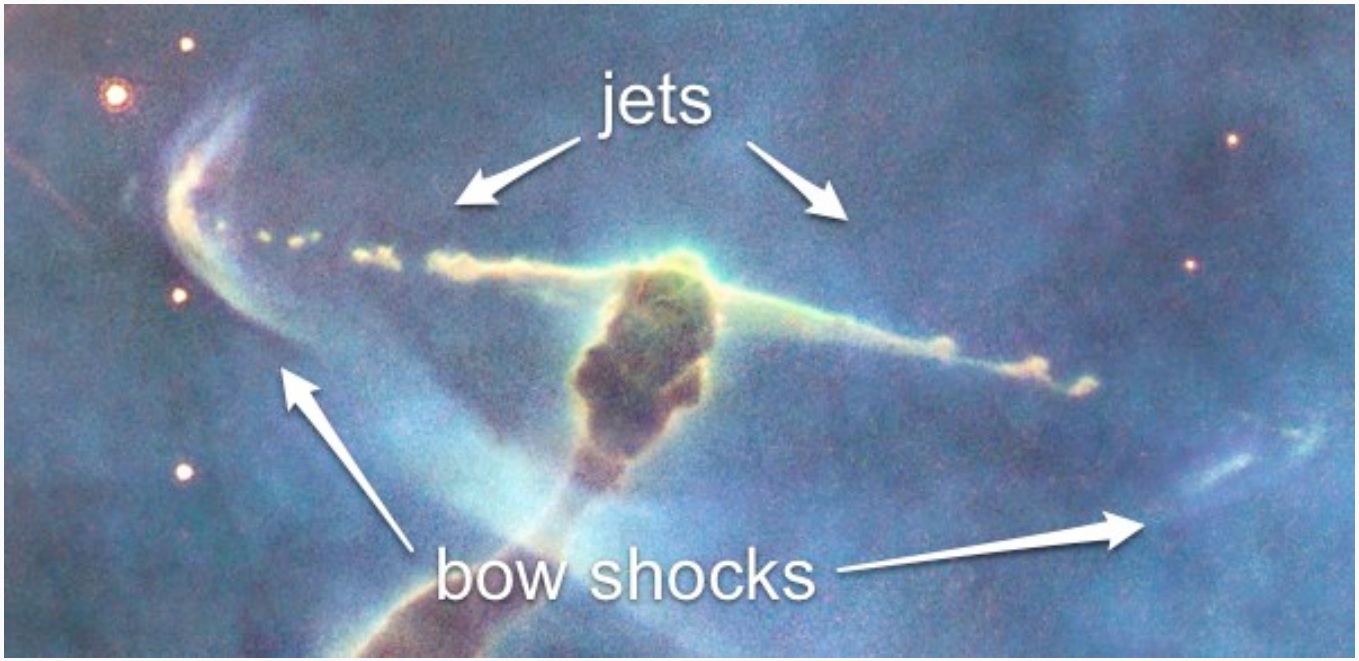

Non-thermal (synchrotron) emission from protostellar jets

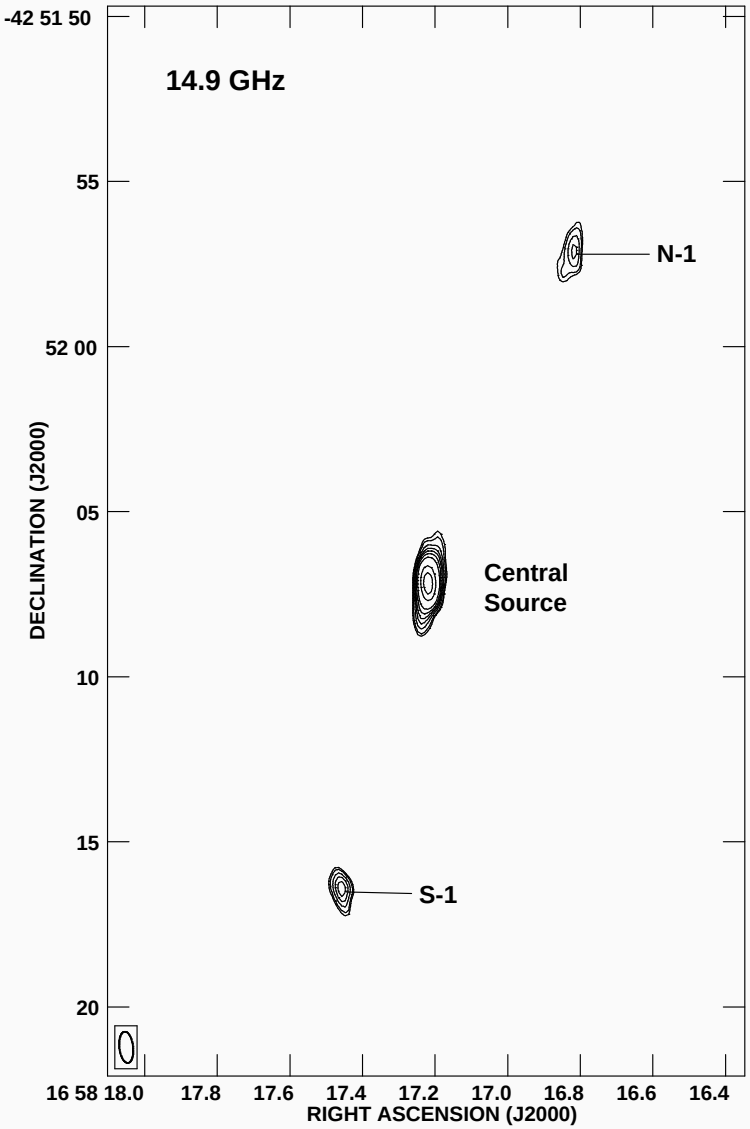

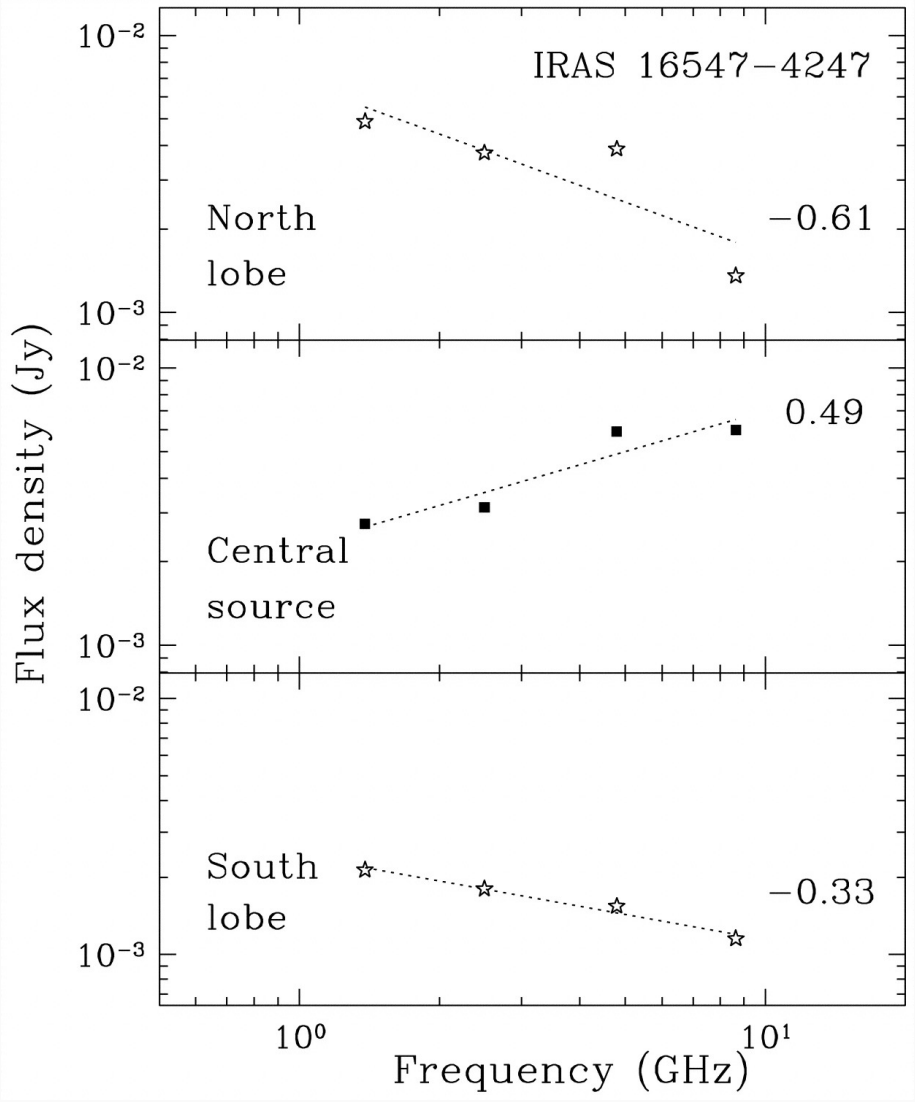

Rodríguez et al. (2005)

Garay et al. (2003)

Magnetic fields and non-thermal particles content

$$\frac{E_e}{\mathrm{GeV}} \sim 2 \times 10^{-7} \left(\frac{\nu}{\mathrm{GHz}}\right)^{\frac{1}{2}} \left(\frac{B_\mathrm{d}}{\mathrm{mG}}\right)^{-\frac{1}{2}}$$

$$\frac{U_\mathrm{e}}{\mathrm{erg\,cm^{-3}}} \sim 10^{-8} \left(\frac{\epsilon_{\mathrm{syn},\nu}}{\mathrm{erg\,cm^{-3}}}\right) \left(\frac{\nu}{\mathrm{GHz}}\right)^{\frac{s-1}{2}} \left(\frac{B_\mathrm{s}}{\mathrm{mG}}\right)^{-\frac{s+1}{2}}$$

$$\eta_\mathrm{p} = \frac{U_\mathrm{p}}{2 m_\mathrm{p} n_\mathrm{i} v_\mathrm{sh}^2} \approx 0.1 \left(\frac{U_\mathrm{p}}{10^{-6}\,\mathrm{erg\,cm^{-3}}}\right) \left(\frac{n_\mathrm{i}}{10^3\,\mathrm{cm^{-3}}}\right)^{-1} \left(\frac{v_\mathrm{sh}}{500\,\mathrm{km\,s^{-1}}}\right)^{-2}$$

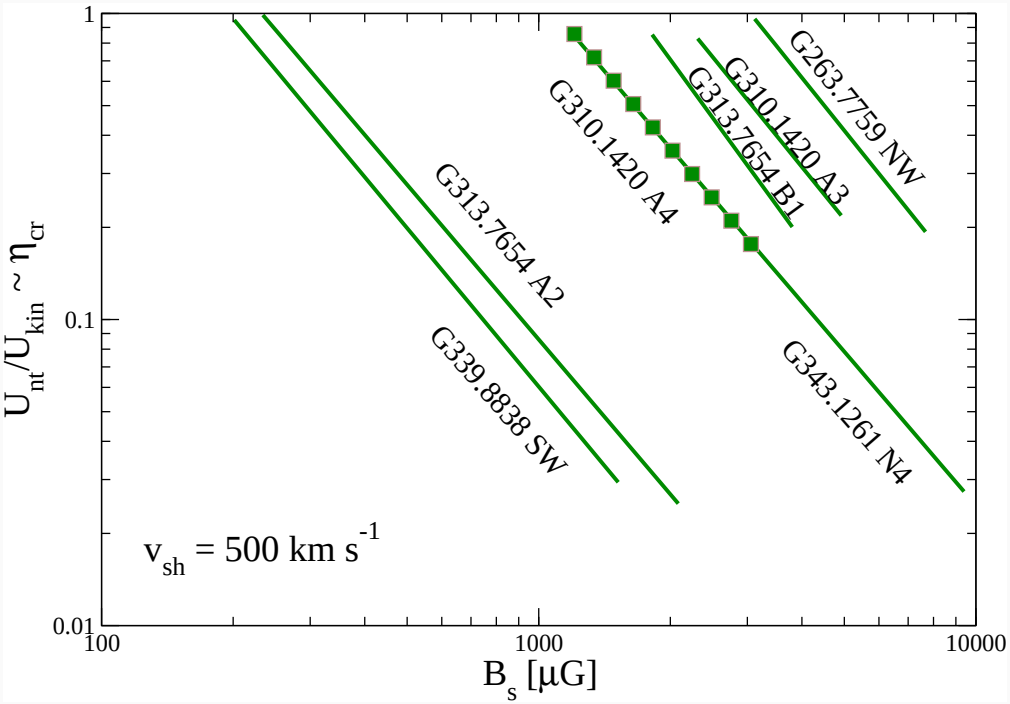

Araudo et al. (in prep.)

$$U_p = a U_e$$

$$a = \left(\frac{m_\mathrm{p}}{m_\mathrm{e}}\right)^{\frac{3-s}{2}}$$

$$U_\mathrm{nt} = U_e + U_p$$

Driving term:

$$\boxed{\zeta = \eta_p \frac{V_\mathrm{sh}}{c}}$$

Cosmic-ray streaming instabilities in partially ionized plasma

$$\zeta M_{\rm A}^2 \simeq 1.8\times10^3 \left(\frac{\eta_p}{0.01}\right)\left(\frac{n_i}{10^3{\rm cm}^{-3}}\right)\left(\frac{B_{\rm j}}{\mu{\rm G}}\right)^{-2}\left(\frac{v_{\rm sh}}{500\,{\rm km\,s}^{-1}}\right)^3$$

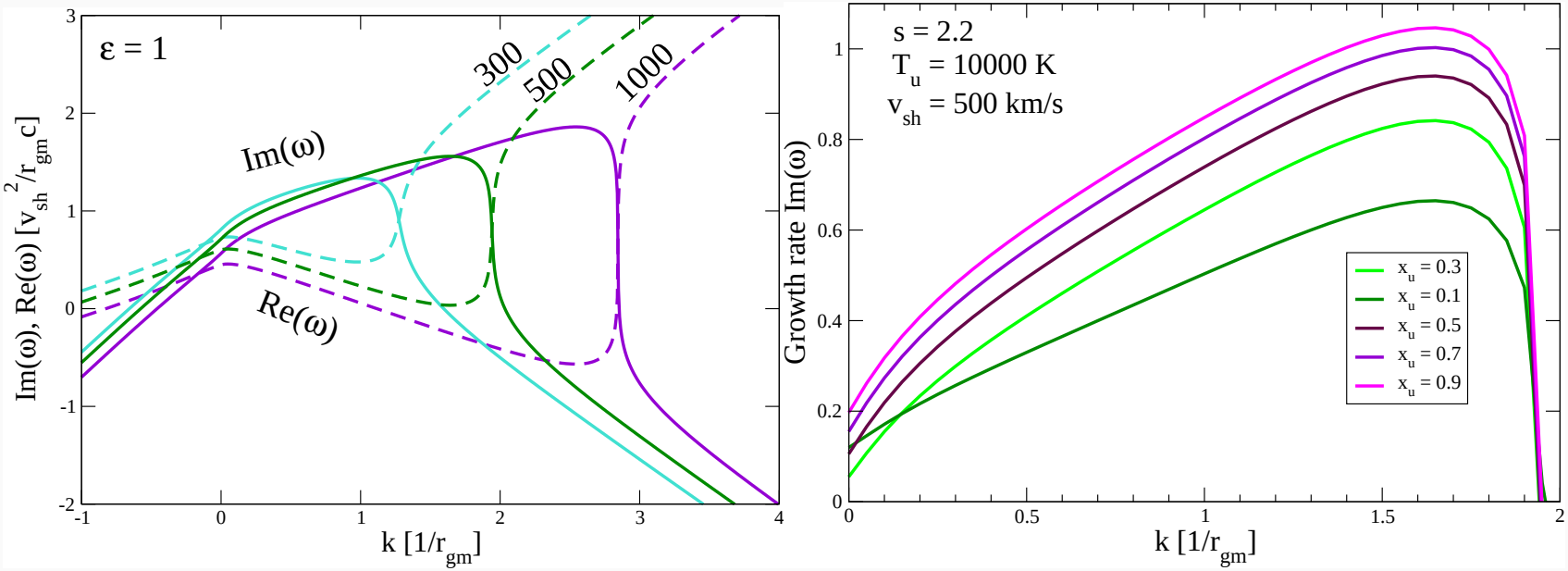

Araudo et al. (in prep.)

Electrons maximum energies

- Electrons maximum energy is determined by synchrotron cooling and escape downstream

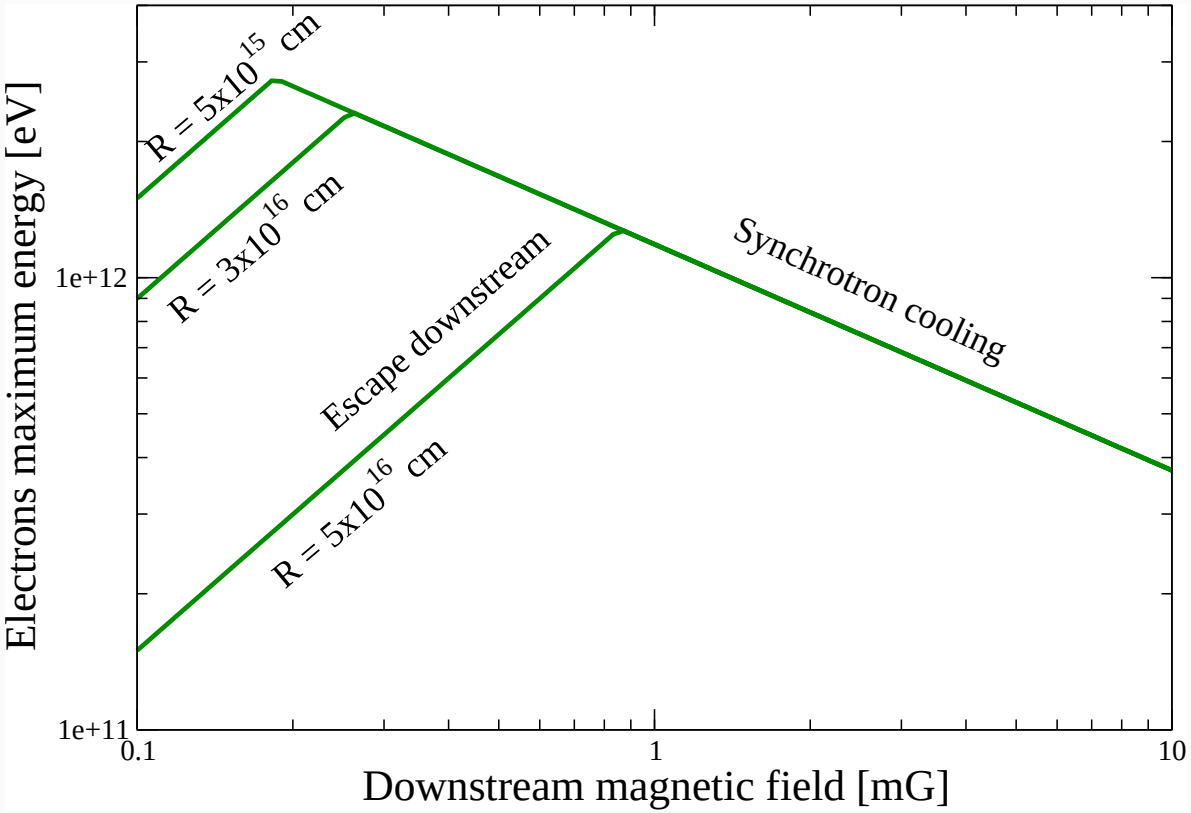

Protons maximum energies

Protons maximum energy upper-limit due to the escape of particles upstream of the shock (Bell et al. 2013)

$$s > 2 : \frac{E_{p,\max}}{\mathrm{TeV}} \sim \left[(s-2) \left(\frac{\eta_{\mathrm{esc}}}{0.01} \right) \left(\frac{v_{\mathrm{sh}}}{1000\,\mathrm{km\,s^{-1}}} \right)^2 \left(\frac{n_i}{10^3\,\mathrm{cm^{-3}}} \right)^{\frac{1}{2}} \left(\frac{R}{10^{16}\,\mathrm{cm}} \right) \right]^{\frac{0.}{s-}}$$

$$s < 2 : \frac{E_{p,\max}}{\mathrm{TeV}} \sim (2-s) \left(\frac{\eta_{\mathrm{esc}}}{0.01} \right) \left(\frac{v_{\mathrm{sh}}}{1000\,\mathrm{km\,s^{-1}}} \right)^2 \left(\frac{n_i}{10^3\,\mathrm{cm^{-3}}} \right)^{\frac{1}{2}} \left(\frac{R}{10^{16}\,\mathrm{cm}} \right)$$

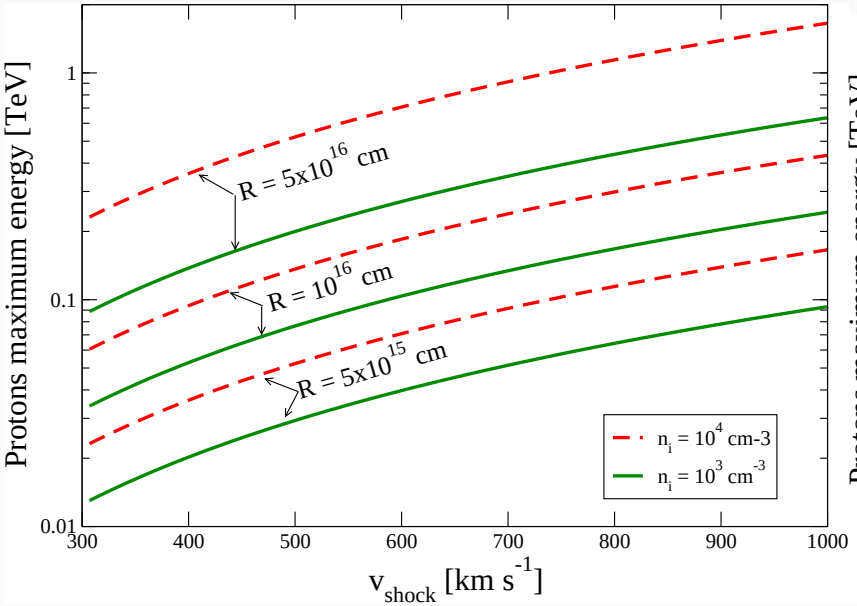

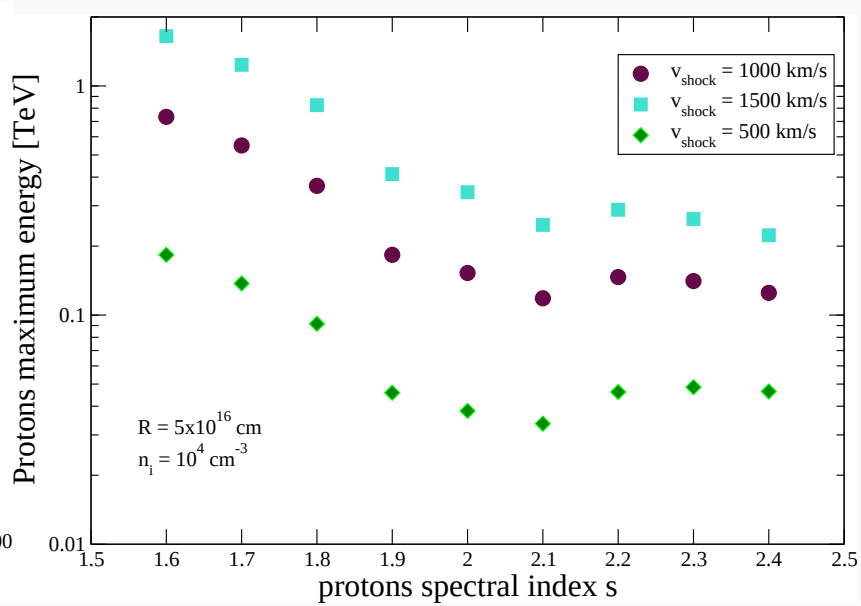

Gamma-ray emission

- GeV-TeV protons produce gamma-rays by proton-proton collisions in the molecular cloud
- Rayleigh-Taylor mixing in the contact discontinuity will increase the density in the reverse shock downstream region

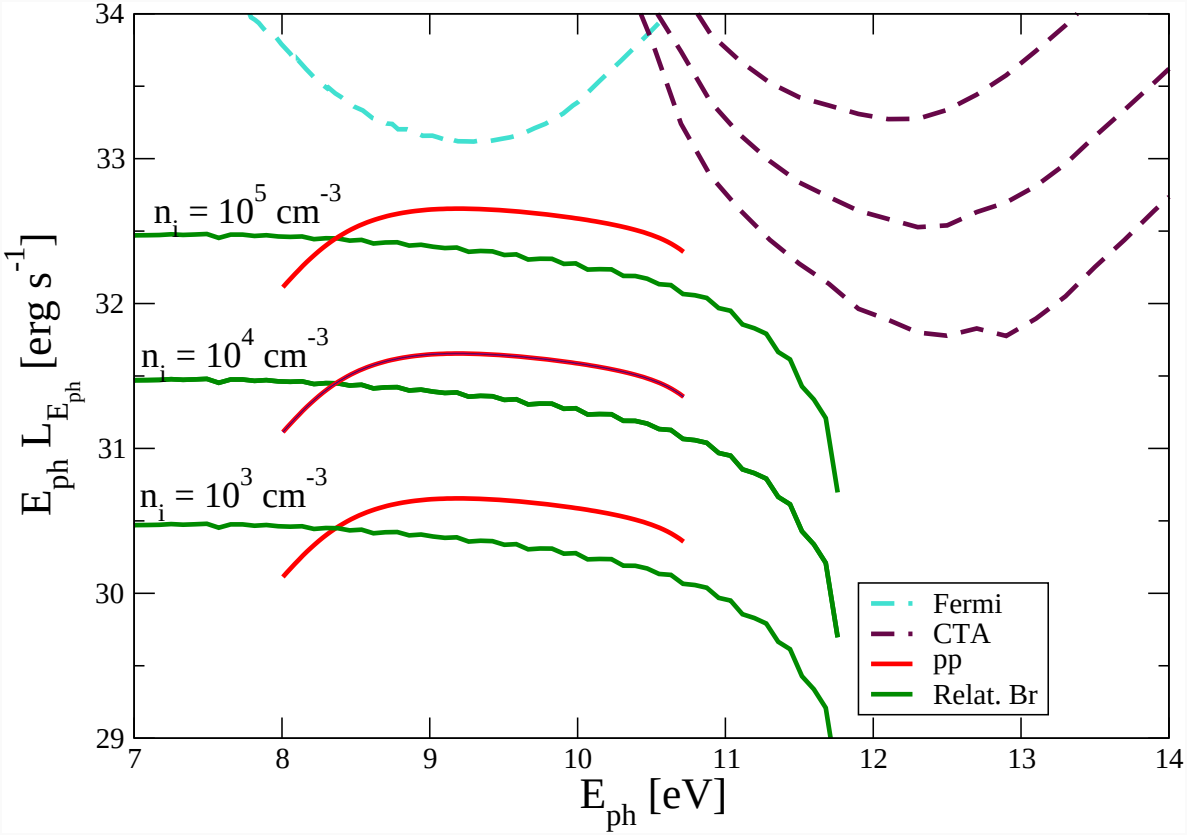

Model for the source IRAS 16547-4247, located at $d = 2.9$ kpc

Laser experiments

Protostellar jets have been well studied in laser experiments

- Collisionless shocks with velocities $\sim$ 1700 km/s have been created in the lab (talk by F.Fiuza)
- Magnetic fields and jet collimation (e.g. Albertazzi et al. 2014)
- Bell instabilities?

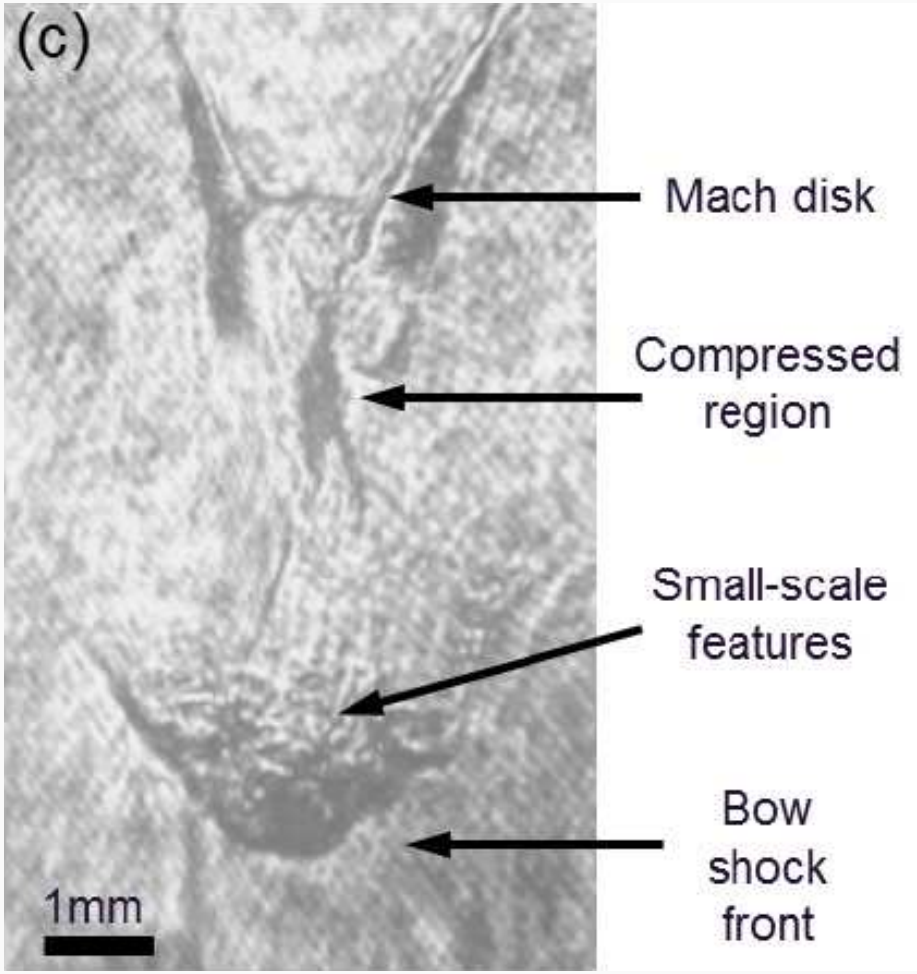

Suzuki-Vidal et al. 2015

Conclusions

- Jets from high mass protostars are synchrotron radio emitters
- Magnetic fields inferred from the synchrotron emission are about 100 μG $\gg B_{\rm jet,nt} \sim 1$ μG (e.g. Hartigan et al. 2007)
- The energy density in relativistic protons (U_p) is high enough to excite the Bell instability and therefore ....

    1. amplify the magnetic field
    2. Bell modes remain in partially ionized plasmas (Reville et al. 2007)

- The maximum energy of electrons and protons is $\sim$ TeV
- High Mass protostellar jets are excellent targets for CTA

The detection of gamma rays from protostellar jets will be very important to study **diffusive shock acceleration** and **magnetic field amplification** in the high-density ($n_{\rm j} \sim 100 - 10^4$ cm^{-3}) and low-velocity ($v_{\rm j} \sim 500$ km s^{-1}) regime

Fermi data

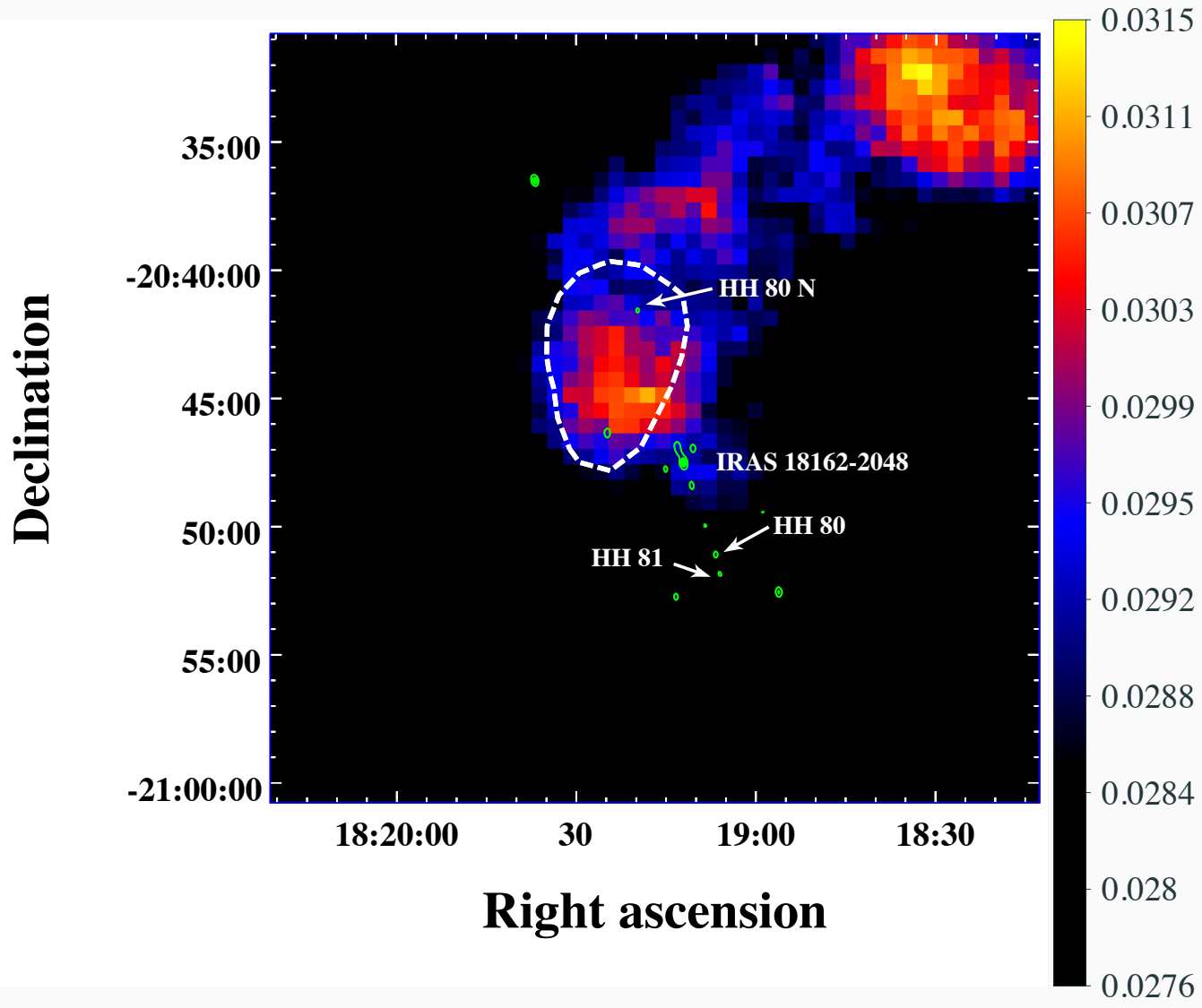

Courtesy of D. Castro

Jet termination shocks

Thermal cooling length:

$$d_{\rm th}^{\rm j,mc} \sim 2 \times 10^{14} \left(\frac{n_{\rm j,mc}}{100\,{\rm cm}^{-3}} \right)^{-1} \left(\frac{v_{\rm rs,bs}}{100\,{\rm km\,s}^{-1}} \right)^{4.5} \ {\rm cm}$$

- Radiative bow shocks:
  $d_{\rm th,mc} < r_{\rm j}$
- Adiabatic reverse shocks:
  $d_{\rm th,j} > r_{\rm j}$

Particle acceleration in reverse shocks!

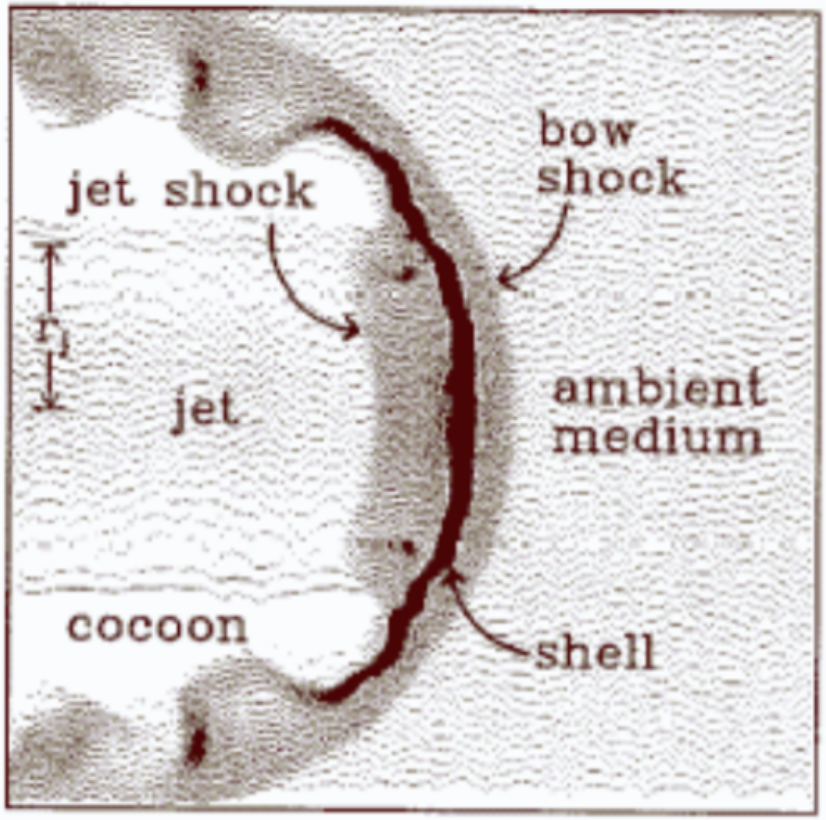

Blondin et al. (1889)

Magnetic fields

Scalling law $B_j \propto n_j^{\beta}$
$0.5 < \beta < 1$

AVERAGE JET PARAMETERS

Distance from Star (AU)	Arcseconds[a]	n[b] (cm^{-3})	$B_\perp$	V_A[c] (km s^{-1})
10	0.02	2.5×10^6	82 mG	113
30	0.06	1.5×10^6	53 mG	94
100	0.2	4.5×10^5	19 mG	62
300	0.6	8.8×10^4	4.8 mG	35
10^3	2.2	10^4	0.75 mG	16
3×10^3	6.5	1.2×10^3[d]	124 μG[d]	7.8
10^4	22	110[d]	16 μG[d]	3.3
3×10^4	65	12[d]	2.4 μG[d]	1.5

Hartigan et al. (2007)

Equipartition magnetic fields in synchrotron jets: $B_{eq} \sim 100 - 500\,\mu$G $\Rightarrow B_{eq} \sim 100 B_j \Rightarrow$ Magnetic field amplification?

$B_{eq} \sim 100\,\mu\text{G} \Rightarrow U_p > U_e \sim 10^{-8}(B_{eq}/500\,\mu\text{G})$ erg cm$^{-3} \Rightarrow$ Local particle acceleration! (Padovani et al. 2016, Fontani et al. 2017)

HH 81 (Radio + X-rays)

Shift between radio and X-ray emission (peak possition)

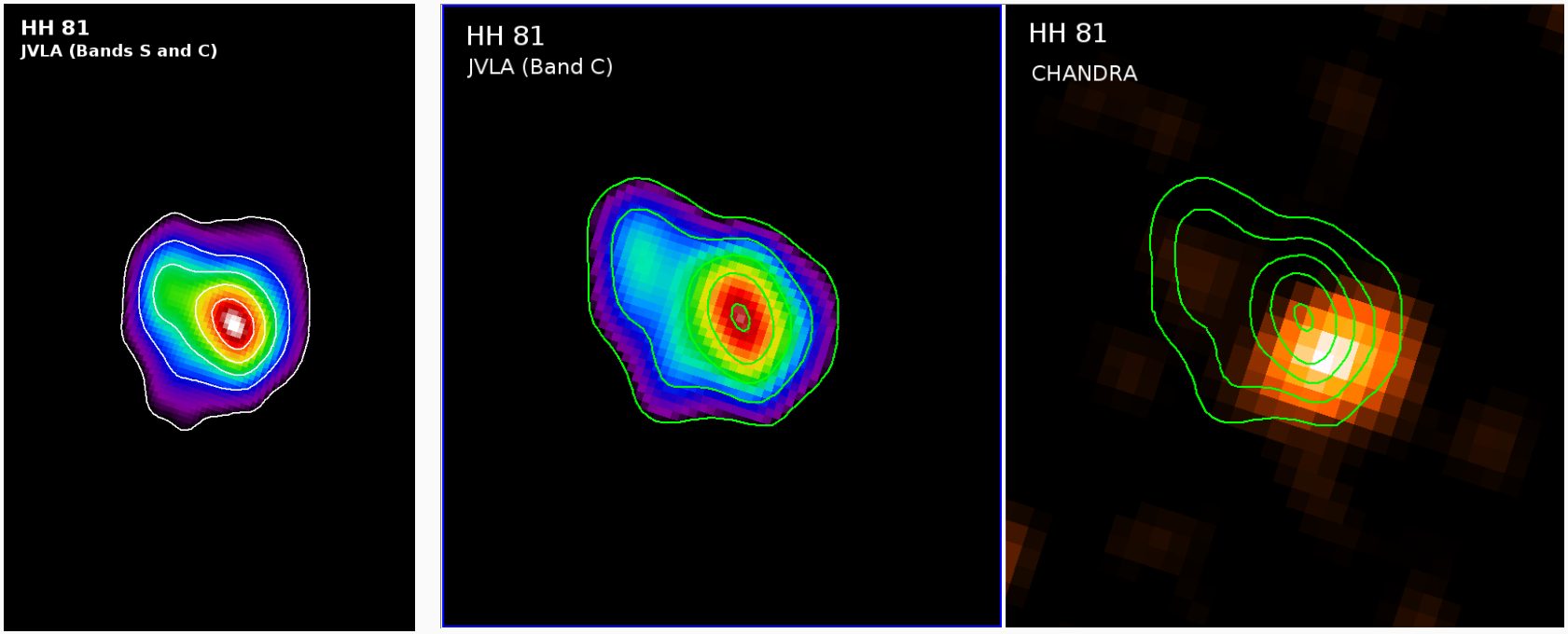

Rodríguez-Kamenetzky et al. (2019)

HH 80 (Radio + X-rays)

Shift between radio and X-ray emission (peak possition)

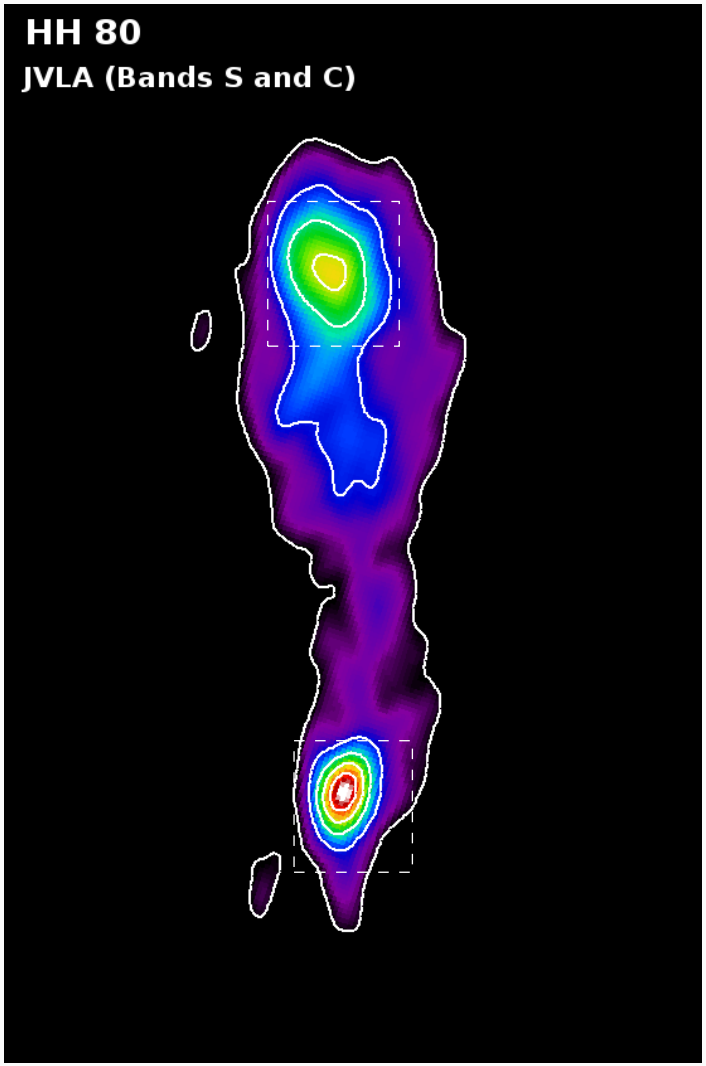

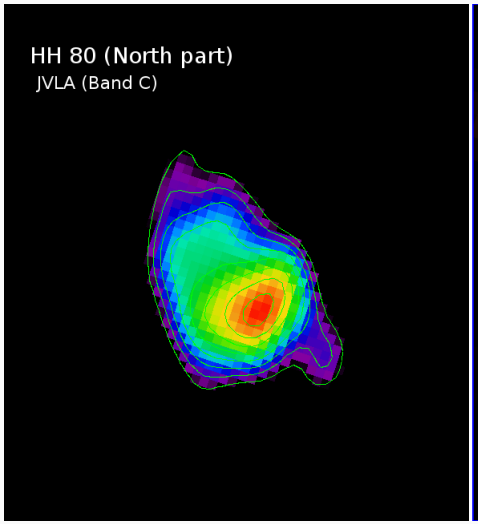

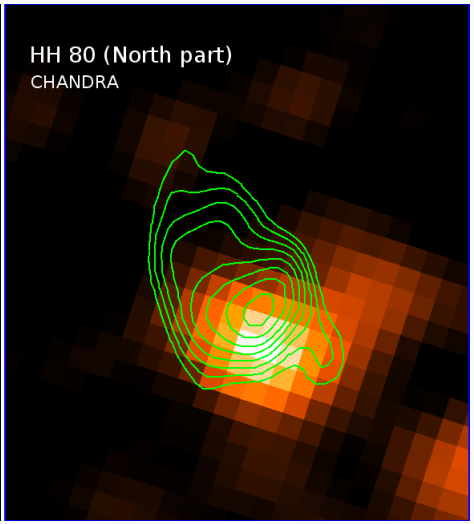

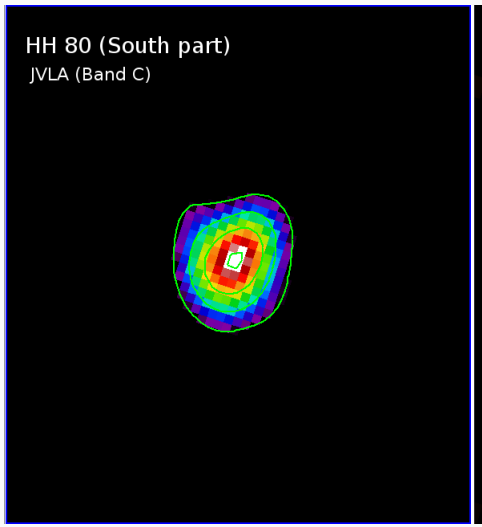

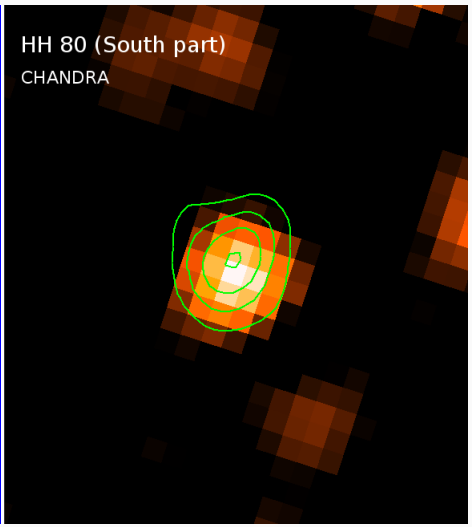

Rodríguez-Kamenetzky et al. (2019)

Polarization measurements

Polarization measurement in IRAS 18162 (Herbig-Haro objects HH80 and HH81)

- Low spatial resolution VLA data (C-configuration)
- Magnetic field parallel to the jet axis
- Equipartition magnetic field $\sim$ 0.2 mG

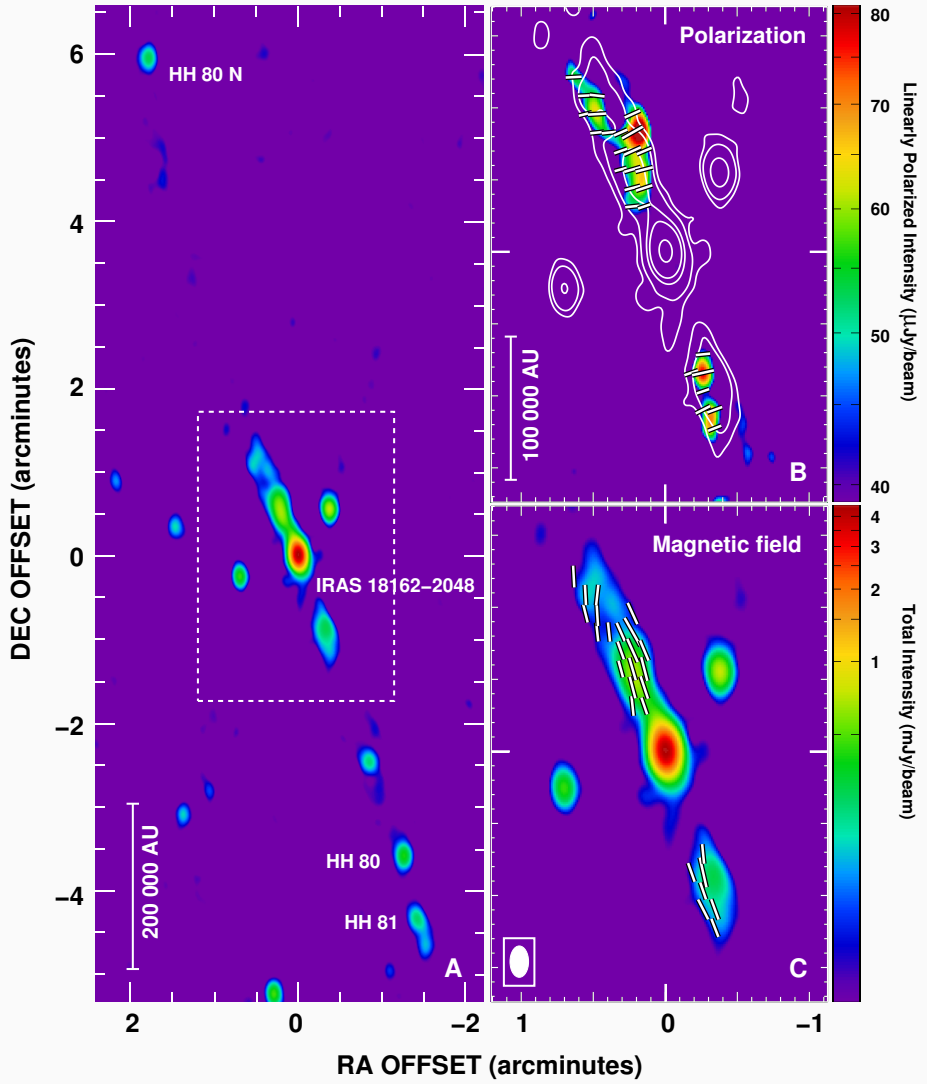

Carrasco-Gonzalez et al. (2010)

Shocks in YSO jets

Internal shocks formed by variations in the jet velocity (Raga et al. 1990)

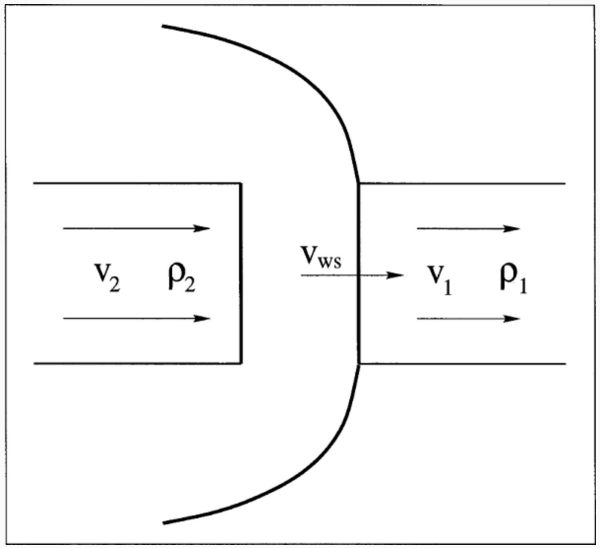

Cantó et al. (2000)

Clumpy jets: chains of subradial clumps propagating through a moving interclump medium

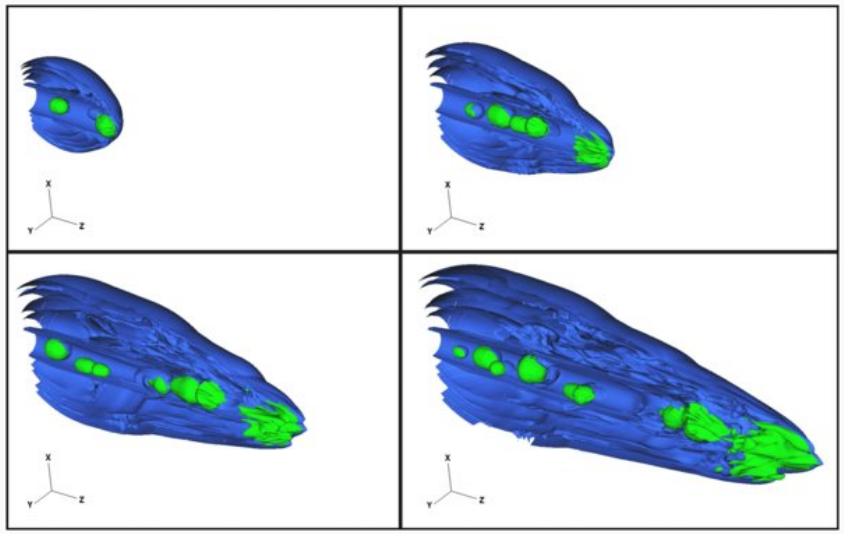

Yirak et al. (2009)

DSA in partially ionized plasmas

Ionization and Coulomb losses can be important before injection.
The acceleration processes at these energies has to be fast.

- $v_{\rm sh} = 10000$ km/s
- $n_{\rm H} = 10^9$ cm^{-3}
- $x_i = 0.99$
- $B = 1$ mG

Also....
damping of Alfven scattering waves by ion-neutral collisions

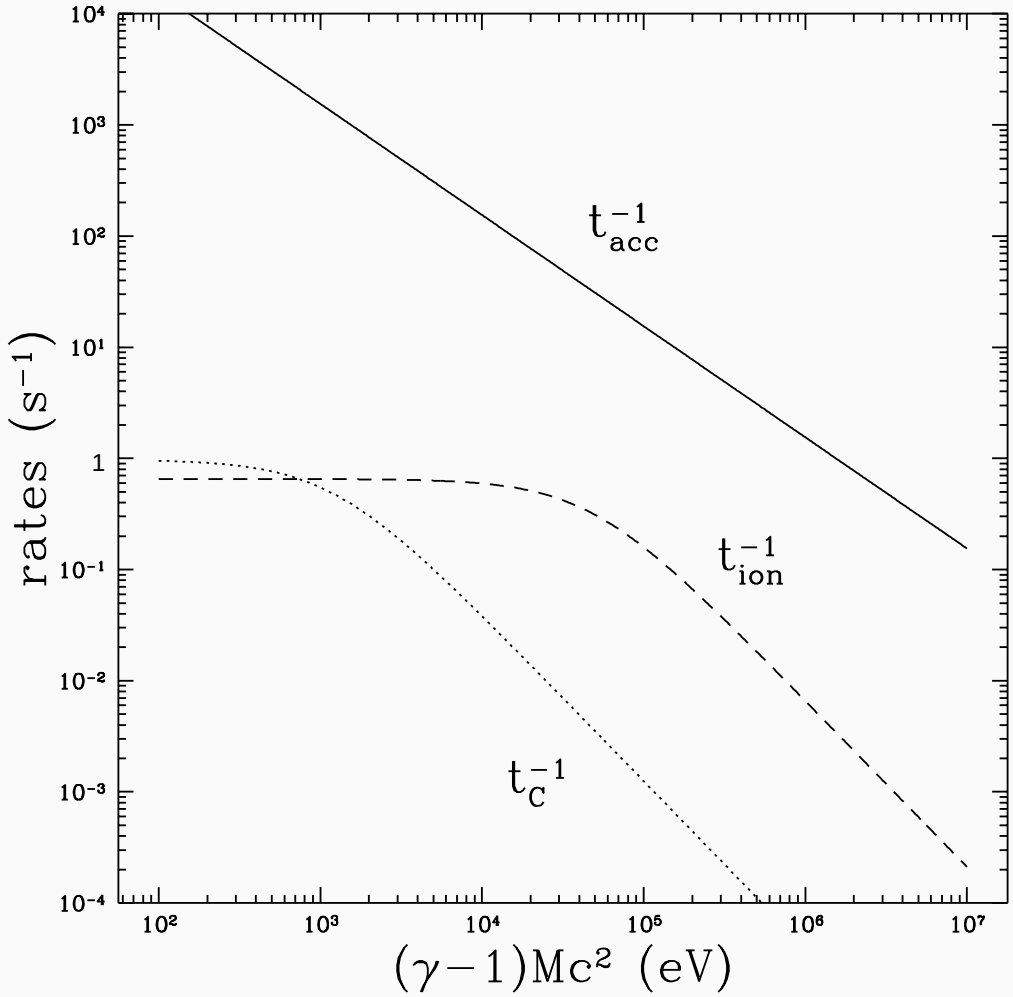

Drury et al. (1996)

Maximum energy of non-thermal particles

- Bell (non-resonant)

$$\Gamma_{\rm max-NR} \sim \eta_{\rm cr} M_{\rm A}$$

- Alfvén (resonant)

$$\Gamma_{\rm max-RES} \sim r_{\rm g}^{-1} \sqrt{\frac{\eta_{\rm cr} V_{\rm sh}^3}{c}}$$

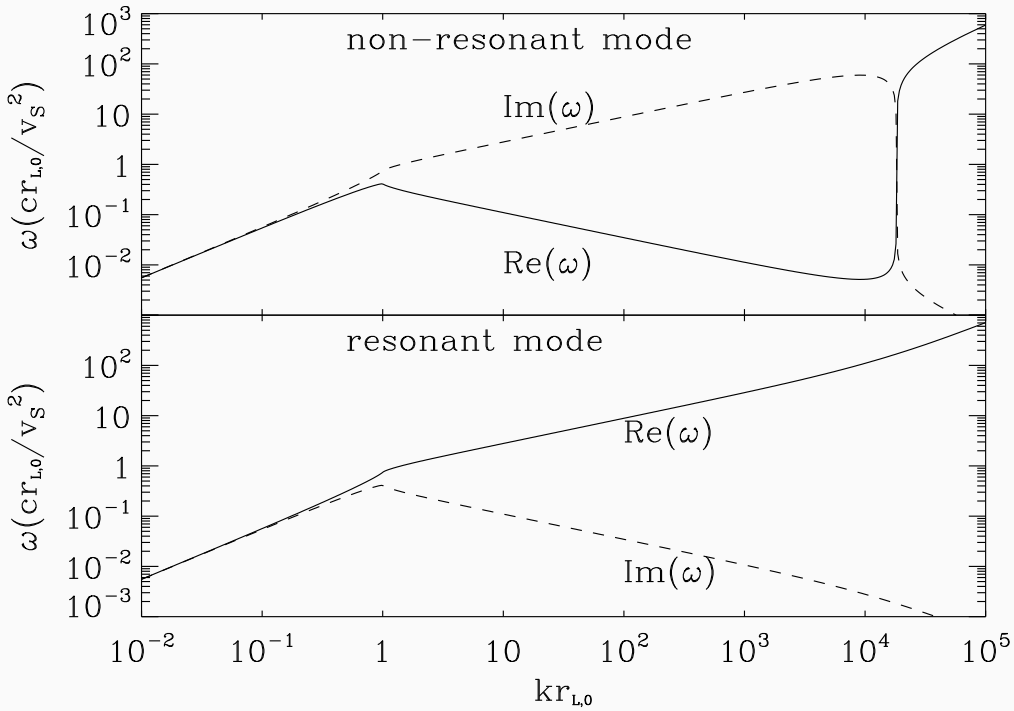

Amato & Blasi (2009)

$$\boxed{\Gamma_{\rm max-NR} > \Gamma_{\rm max-RES}}$$

$t_{\rm acc} \sim \frac{1}{\Gamma_{\rm max}} \Rightarrow$ in the Bell regime particles achieve higher energies in the available time

Cosmic-ray streaming instabilities

Dispersion relation

$$\omega^2 - k^2 v_{\rm A}^2 - k\zeta \frac{v_{\rm sh}^2}{r_{\rm gm}} = 0$$

- Alfvén (resonant): $k^2 v_{\rm A}^2 > k\zeta \frac{v_{\rm sh}^2}{r_{\rm gm}}$
- Bell (non resonant): $k^2 v_{\rm A}^2 < k\zeta \frac{v_{\rm sh}^2}{r_{\rm gm}}$

  Magnetic field amplification!

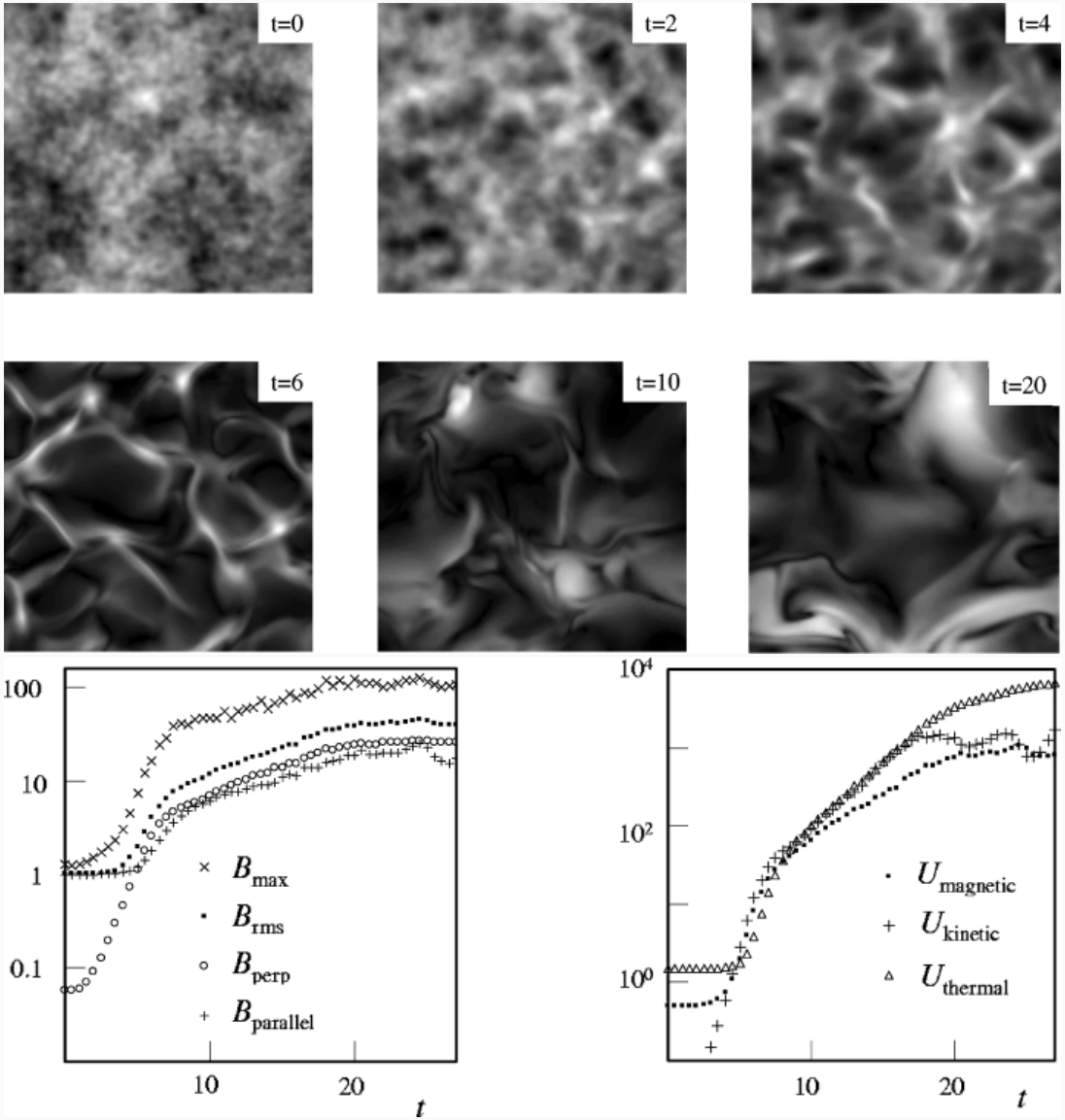

Bell (2004, 2005)

Ion-neutral damping

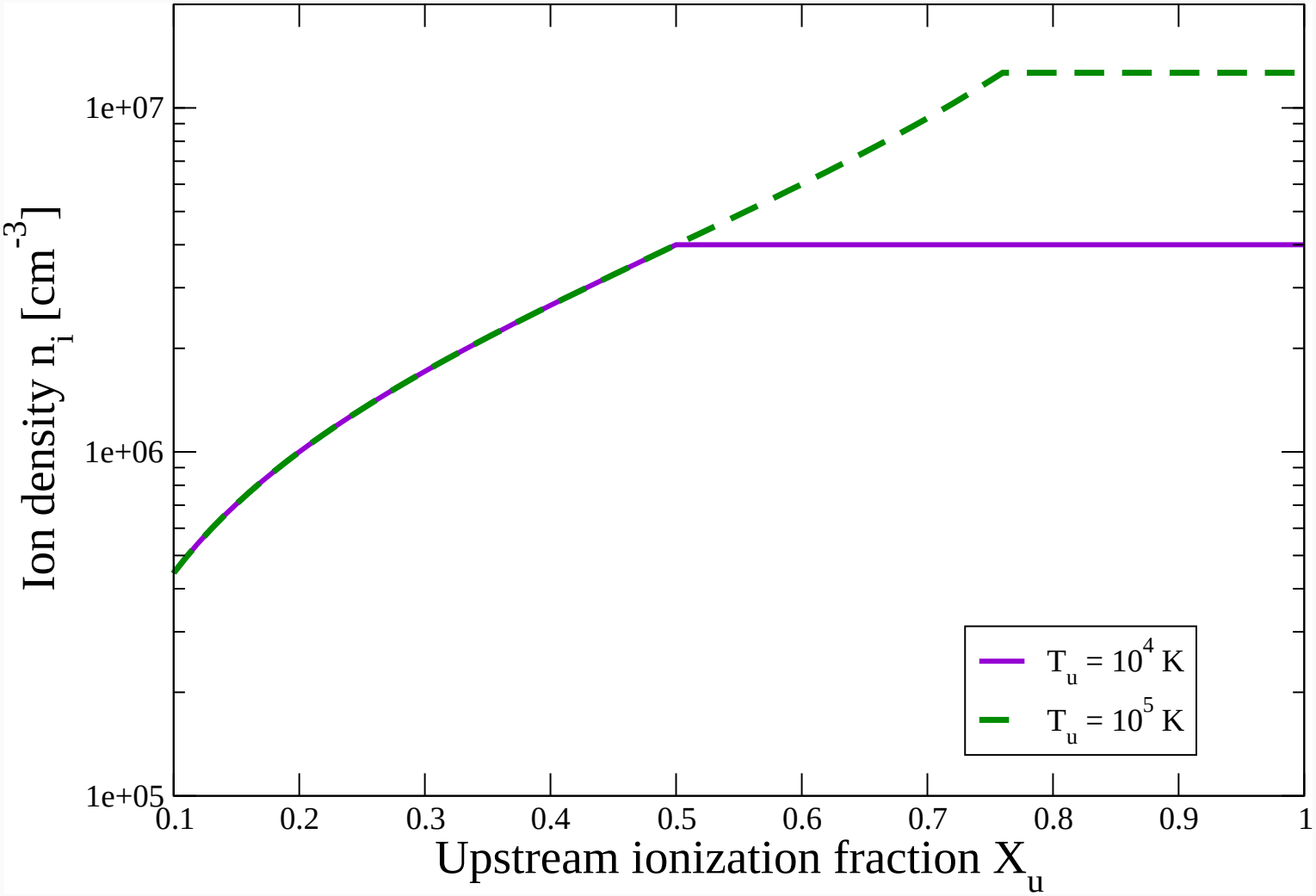

Bell instabilities are not damped in partially ionized plasmas

- Solid
  $n = 0.1\ \mathrm{cm}^{-3}$,
  $T = 10^4\ \mathrm{K}$
- Dashed
  $n = 1\ \mathrm{cm}^{-3}$,
  $T = 10^3\ \mathrm{K}$
- Dot-dashed
  $n = 10\ \mathrm{cm}^{-3}$,
  $T = 10^2\ \mathrm{K}$

Maximum growth rate $\Gamma_{\max}$

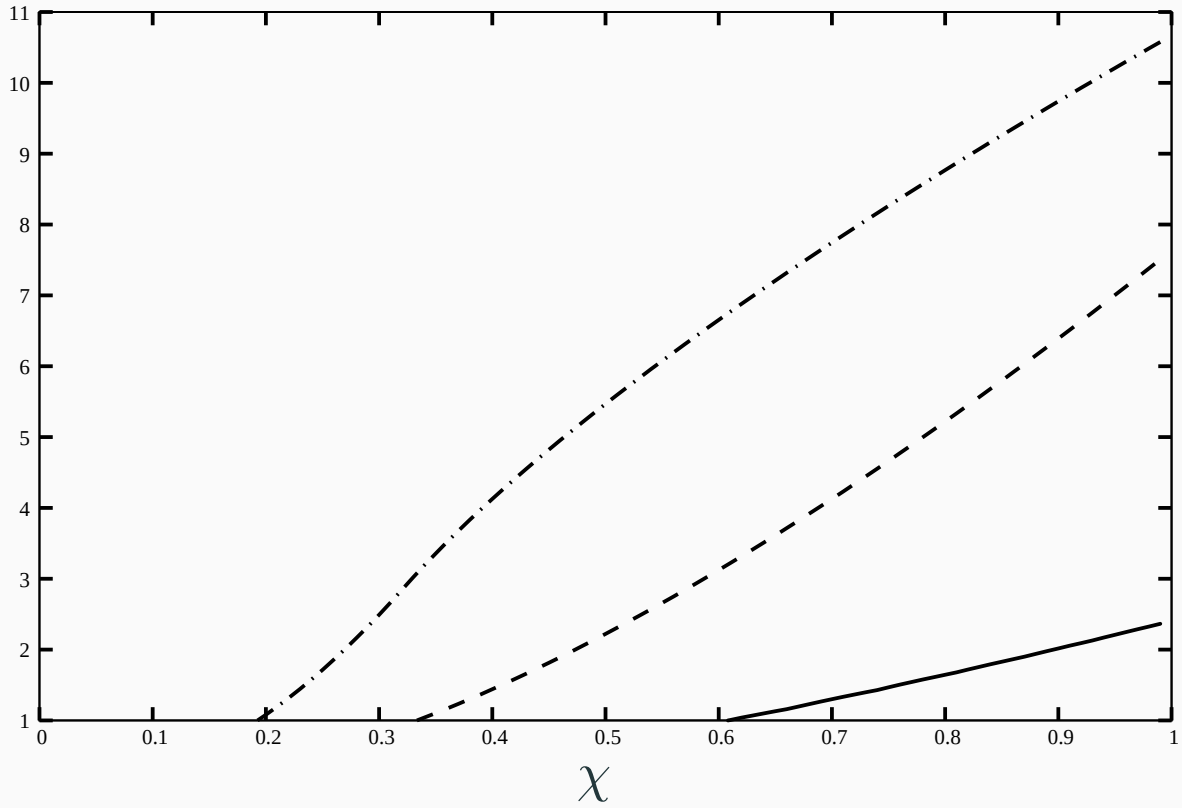

Reville et al. (2007)

Bell-Alfvén transition regime

Saturation magnetic field: $U_{\rm mag} \sim U_p \left(\frac{v_{\rm sh}}{c}\right)$

$$\frac{B_{\rm sat}}{100\,\mu{\rm G}} \sim \left(\frac{U_p}{10^{-7}\,{\rm erg\,cm^{-3}}}\right)^{\frac{1}{2}} \left(\frac{v_{\rm sh}}{500\,{\rm km\,s^{-1}}}\right)^{\frac{1}{2}}$$

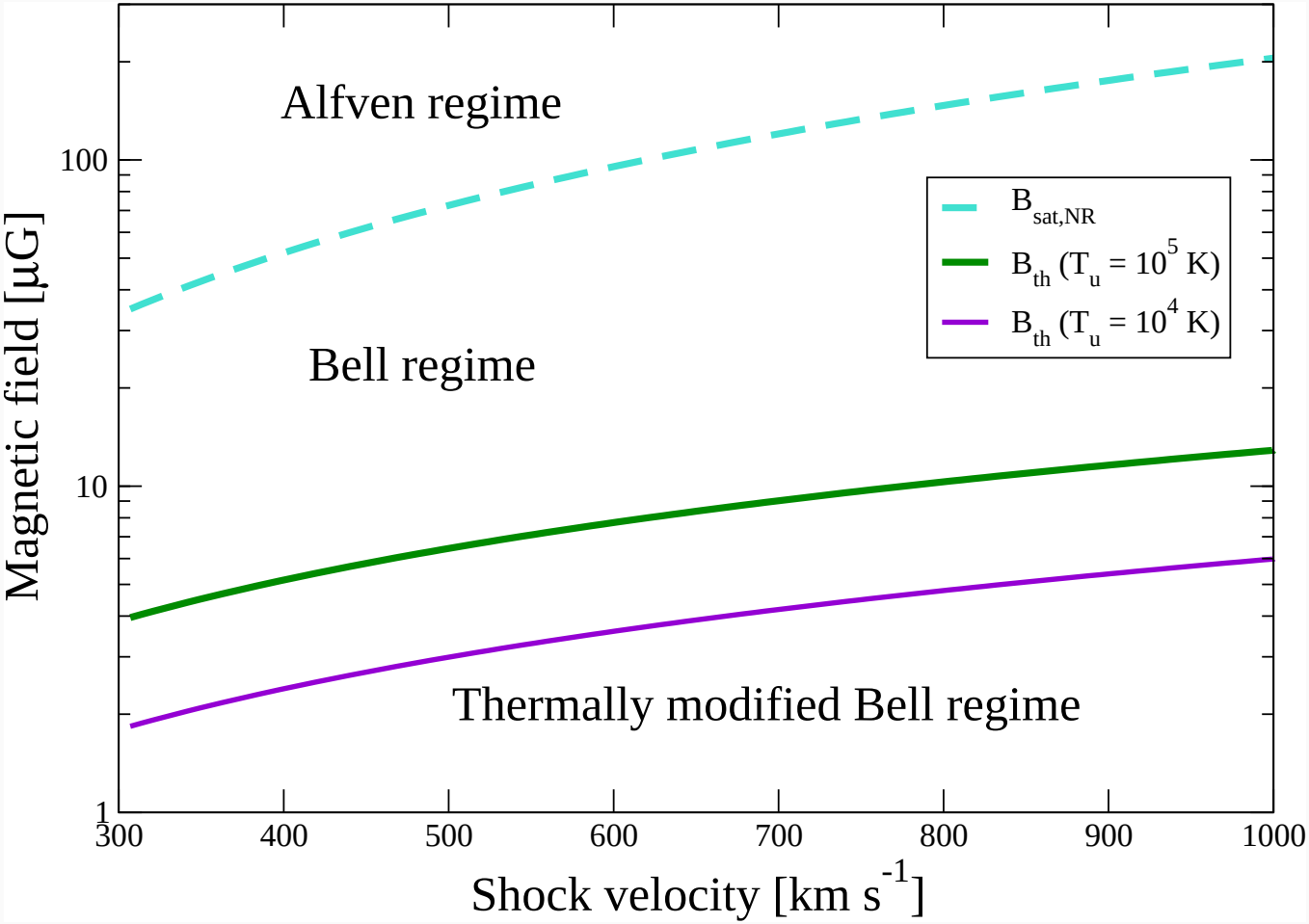

Cosmic-ray streaming instabilities in partially ionized plasma

$$\omega^3 + i\omega^2\nu_{\rm in}\left(\frac{1}{1-X_{\rm u}}\right) + \omega A + i\nu_{\rm in}\left(\frac{X_{\rm u}}{1-X_{\rm u}}\right)A = 0$$

$$\sigma(X,s) = \frac{3}{4}\left(\frac{x^{-3}}{s-6} - \frac{x^{-1}}{s-4}\right)\log\left|\frac{x+1}{x-1}\right| - \frac{3x^{-2}}{2(s-6)} + \frac{3}{2(s-3)}\left(\frac{1}{s-6} - \frac{1}{s-4}\right) \times$$

$$\left\{\mathrm{Re}\left[{}_2\mathrm{F}_1\left(\frac{3-\mathrm{s}}{2}, 1, \frac{5-\mathrm{s}}{2}, \frac{1}{\mathrm{x}^2}\right)\right] - 1\right\} + \frac{3\pi}{4}i\epsilon\begin{cases} \frac{x^{-3}}{s-6} - \frac{x^{-1}}{s-4} & X > 1 \\ \frac{x^{3-s}}{s-6} - \frac{x^{3-s}}{s-4} & X \leq 1, \end{cases}$$

$$\frac{\nu_{\rm in}}{\mathrm{s}^{-1}} \simeq 8.9\times10^{-9}\left(\frac{T_{\rm u}}{10^4\ \mathrm{K}}\right)^{0.5}\left(\frac{n_{\rm n}}{\mathrm{cm}^{-3}}\right)$$

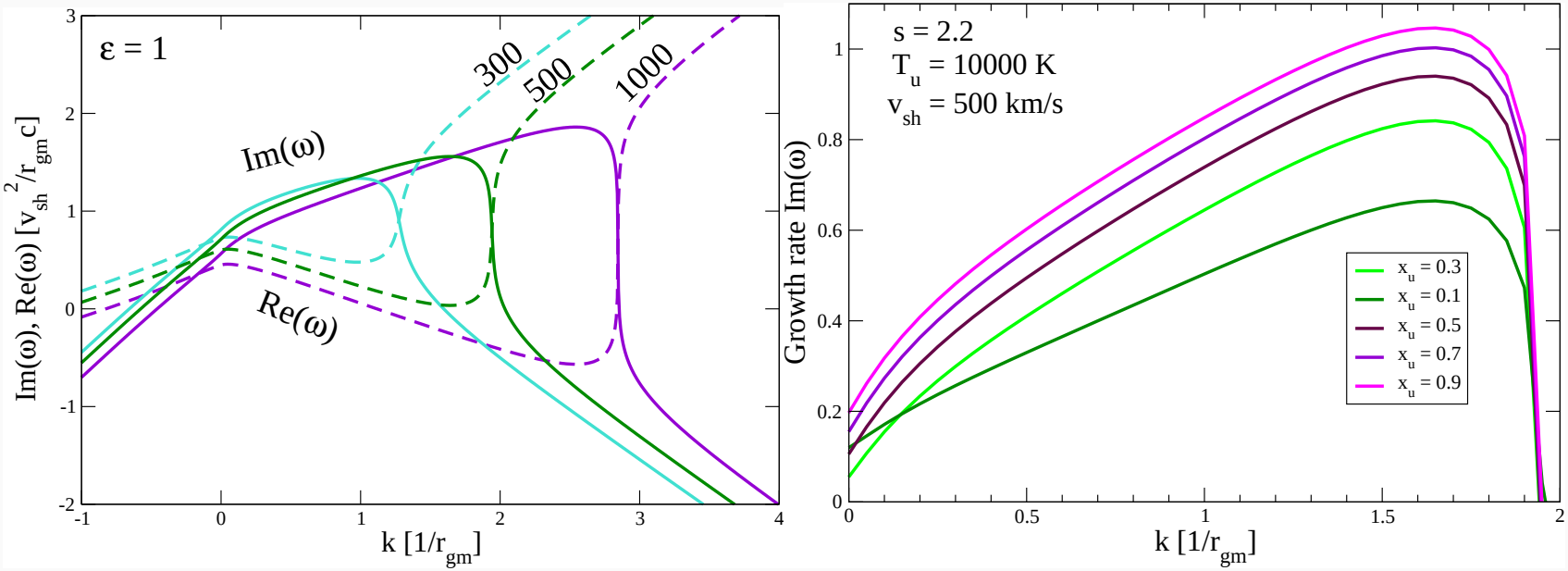

Araudo et al. (in prep.)